

Investigating an upwelling system along the eastern Makran coast

M. ZOLJOODI ZARANDI¹, A. BARZANDEH², S. HASSANZADEH³ AND R. ZOLJOODI ZARANDI⁴

¹ Department of Marine Meteorology & Physical Oceanography, Atmospheric Science and Meteorological Research Center (ASMERC), Tehran, Iran

² Department of Marine Systems, Tallinn University of Technology, Tallinn, Estonia

³ Faculty of Physics, University of Isfahan, Isfahan, Iran

⁴ Department of Industrial Engineering, K.N. Toosi University of Technology, Tehran, Iran

(Received: 30 March 2023; accepted: 10 November 2023; published online: 1 March 2024)

ABSTRACT The study investigated wind-driven upwelling along the Makran coasts, utilising wind, temperature, and sea surface current data. Results revealed a seasonal coastal upwelling system along the eastern Makran coasts, primarily influenced by coastline orientation, and impacting sea surface dynamics. Trend analysis of sea surface temperature (SST) data indicated consistently negative, or near-zero, SST variations in the Makran upwelling system, in contrast to adjacent areas. Peak upwelling intensity occurred in May, spanning 62° to 66° E, encompassing over 300 km of Makran coasts. Temperature profile data validated the presence of a seasonal coastal upwelling system along the eastern Makran coasts. The examination of sea surface current components, in the northern Arabian Sea and the Gulf of Oman, highlighted the dominance of the seasonal upwelling system, driven by a decreased geostrophic current in May. In the northern Arabian Sea, the intensified geostrophic current, interacting with the Ekman current, diminished coastal upwelling intensity along the eastern Makran coasts.

Key words: coastal upwelling, Makran coasts, SST, seasonal variabilities.

1. Introduction

Makran coastal waters are located at a latitude of approximately 25° N, spanning from a longitude of 57° to 67° E. This area encompasses the northern coastlines of the Gulf of Oman and the northernmost coastlines of the Arabian Sea (Fig. 1). Here, the Indian monsoon climate significantly influences regional oceanic and atmospheric circulation (Murtugudde *et al.*, 2007; Al-Azri *et al.*, 2010; Eshghi *et al.*, 2020). During the summer monsoon season (May - September), eastward sea surface currents prevail, while during the winter monsoon season (November - February), westward sea surface currents dominate in the central Arabian Sea (Findlater, 1969; Shankar *et al.*, 2002). Over the Gulf of Oman and the northern Arabian Sea, the summer monsoon is characterised by persistent and intense south-westerly winds, with an average speed of 15 m/s. Conversely, the winter monsoon features less intensity and is associated with north-easterly winds, with average speeds of less than 5 m/s (Chaichitehrani and Allahdadi, 2018). Shamal winds can also influence circulation patterns in the Gulf of Oman and the northern Arabian Sea. These extratropical climate systems are characterised by strong north-westerly low-level winds that blow over the Arabian peninsula, often extending into the Arabian Sea, and reaching the Makran coasts (Vinod Kumar *et al.*, 2014).

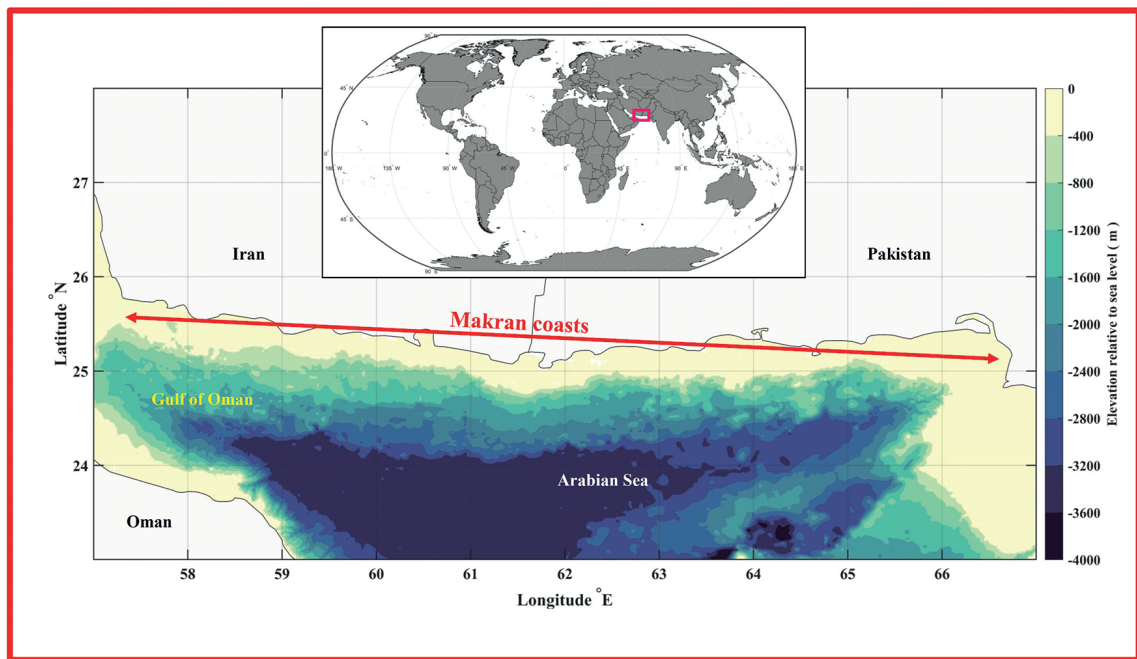


Fig. 1 - The Makran coasts, the study area.

The occurrence of Shamal winds in the Arabian Sea, during the summer, is closely linked to the phenomenon known as break-monsoons, where the monsoonal winds weaken during the dominance of Shamals (Aboobacker *et al.*, 2011; Glejin *et al.*, 2013; Muraleedharan *et al.*, 2013). Circulation in the eastern part of the Gulf of Oman is primarily dominated by a cyclonic gyre. In the western part, an anticyclonic gyre is also dominant; however, the circulation in this region is more complex. From the west, the hydrological regime of the Gulf of Oman is influenced by the influx of high-salinity waters from the shallow Persian Gulf through the Strait of Hormuz (Banse, 1997; Prasad *et al.*, 2001). The Persian Gulf water mass flows along the southern coast of the Gulf of Oman, while the surface water mass of the Indian Ocean is centred near the offshore frontal part of the Makran coasts (Pous *et al.*, 2004). As these dominant circulation patterns, in the Gulf of Oman and the northern Arabian Sea, are primarily concentrated in offshore areas, their impact on coastal water dynamics is expected to be relatively slight. Contrarily, coastal currents can be influenced by external factors (e.g. wind and tides) and may be associated with the circulation prevailing in the region. Previous studies have indicated that tidal currents, in the Gulf of Oman and the northern Indian Ocean, generally, are not intense (Akhyani *et al.*, 2015). However, regional weather conditions, and the interaction of local wind-driven circulation, can give rise to significant patterns of coastal dynamics in the northern Arabian Sea and the Gulf of Oman (Reynolds, 1993; Fritz *et al.*, 2010). A major part of our knowledge of coastal upwelling in the northern Arabian Sea and the Gulf of Oman is based on limited observations and modelling studies carried out in the 1990s and early 2000s. Unfortunately, the lack of observation and concerted modelling efforts resulted in a slow progress of our knowledge of this region over the last couple of decades. The dynamical reasons for the development of multiscale onshore and offshore eddies, and their impact on the coastal upwelling, coastal currents, sea surface temperature (SST), air-sea interactions, and, ultimately, on biology, are still not clear. Thus, considering the importance of this region in regional physical and ecological processes and, most

importantly, its influence on the Indian monsoon, the scientific community should make greater effort to reach a complete understanding of the oceanic processes of this coastal upwelling system (Vinayachandran *et al.*, 2021).

In general, coastal upwelling occurs due to flow divergence, which happens when surface waters are pushed offshore from a coastal boundary by winds blowing parallel to the coast, with the coastline on its left in the northern hemisphere (or on its right in the southern hemisphere). This phenomenon is known as the Ekman transport and is a result of the combination of wind stress and the Coriolis effect caused by the Earth's rotation (Pond and Pickard, 1983). As a result of coastal upwelling, cold waters replace the warm surface waters of the nearshore area. At different time scales, this process has a profound influence on the climate (Bakun, 1990). Globally, there are four major coastal upwelling centres, namely in the Canaries, Benguela, California, and Humboldt. However, compared to the major centres, there are smaller areas with significant patterns of coastal upwelling. Detailed information on coastal upwelling characteristics in these areas could be crucial to aspects of Earth and environmental sciences, as well as to the local economy, given the importance of coastal upwelling in the fishery industries (Watson and Pauly, 2001). The coastal upwelling intensity, in other coastal areas, can be low due to the lack of driving components, such as the eastern boundary currents, though it can still have a significant and undeniable effect on changes in physical and biological properties on regional scales (Lehmann *et al.*, 2012; Barzandeh *et al.*, 2018; Trinchin *et al.*, 2019; Lu *et al.*, 2021).

Depending on regional wind conditions, coastal upwelling systems can either have a quasi-permanent or seasonal nature (Reul *et al.*, 2005; Zavala-Hidalgo *et al.*, 2006). The identification of temporal and spatial characteristics, along coastlines around the world, can be of utmost importance in the recognition of air-sea interactions and climatic consequences. According to the coastal upwelling formation mechanism, one of the factors playing a decisive role in the occurrence of coastal upwelling is the coastline orientation relative to wind direction. Given the variabilities of shoreline angles, on different spatial scales, the manner in which the coastal upwelling intensity is distributed and its effects along a certain shoreline are also significant (Kämpf and Chapman, 2016). Wind-driven coastal upwelling events are typically localised, and coastal upwelling does not occur uniformly along the shorelines. In warm-water ocean regions, the upwelling of colder subsurface waters can result in a reduction of sea surface temperatures, although this process is not necessarily spatially uniform in specific coastal upwelling areas (Tomczak and Godfrey, 2003).

The possibility of coastal upwelling occurrence, in the northern parts of the Gulf of Oman, has been suggested by a number of studies. Reynolds (1993) mentioned that the interface between the two counter-rotating gyres is a region of upwelling along the Iranian coast (the western Makran coasts). The circulation pattern seems to exist in winter and summer, although its strength and upwelling depend on prevailing winds. Johns *et al.* (1999), using limited data over a short period, concluded that the Makran coastal waters present consistent upwelling along the eastern part that is associated with the south-western monsoon. They also stated that the upwelling is more variable along the western parts of the Makran coasts. In addition, they mentioned that, due to spatial and temporal variability in the Makran coastal upwelling system, a better depiction of the winds over the Makran coasts is necessary. According to Kaul *et al.* (2000), the temperature profile differences in some CTD casts, in Makran coastal waters, could be due to an increased upwelling of cold deep waters during the summer. Pous *et al.* (2004) discussed the hydrology and circulation of the Gulf of Oman using data measured over a month, but one of the unanswered questions in their conclusion (a suggestion for further study) concerned the clear identification of upwelling events and their variability. By using Argo profiles, L'Hégaret *et al.* (2013) demonstrated

that upwelling occurs along the western Makran coasts, and downwelling along the Omani coast of the Gulf of Oman, in combination with wind fields. Such upwelling and downwelling processes lead to the presence of colder and fresher waters along the Makran coasts. Using satellite remote sensing, Moradi (2016) revealed that the SST drop along the northern parts of the Gulf of Oman is due to a non-persistent coastal upwelling system, which intensifies from west to east. Ghaemi Bajestani *et al.* (2018), with ArcGIS techniques, and a 3D numerical simulation, indicated the existence of upwelling during the monsoon transition period (October and November) in central parts of the Makran coasts. According to Hassanzadeh and Hosseinibalam (2020), the difference between atmospheric pressure and mean sea level along the Makran coasts is due to alongshore wind stress forcing, and is consistent with that expected from the Ekman dynamics. In addition, Morvan *et al.* (2020) revealed that a local coastal upwelling process, in the western and central Makran coasts, would affect the first 100 m of depth, and Pratik *et al.* (2019) confirmed an upwelling increase in the northern Arabian Sea, consistent with a spatial trend in heat content.

While upwelling events along the Makran coasts have been sporadically reported and studied, a comprehensive and systematic analysis of the spatial and temporal patterns of the Makran coastal upwelling system, is lacking. This study aims to fill this gap by analysing high-resolution satellite data and atmospheric re-analysis, by considering an extended time series (that surpasses previous works) and encompassing the entire Makran coastal area. The primary focus of this research is to investigate the evidence on coastal upwelling occurrences along the Makran coasts using the SST trend, wind-driven coastal upwelling index, temperature profiles, and surface current components, which provide a more comprehensive understanding of the Makran coastal upwelling system.

2. Data and method

To investigate the initial probability of predominant occurrences of coastal upwelling along the Makran coast, 14-year (2007-2020) high-resolution ($5 \times 5 \text{ km}^2$) gridded SST data, with monthly mean time steps, were obtained from the OSTIA global foundation (Good *et al.*, 2020), provided by the Copernicus Marine Environment Monitoring Service¹, and the linear trends of the long-term SST changes were compared with the neighbouring areas. To elaborate further, the SST trend was determined by fitting a linear equation to the SST data time series for each grid point. According to many of the previous studies, among which Chollett *et al.* (2012) and Varela *et al.* (2016), one of the most important pieces of evidence of a coastal upwelling system consists in a locally decreased long-term SST trend. In addition, the coastal upwelling intensity is logically expected to be directly related to the decline rate of the fitted trend line on the SST time series. Nevertheless, the long-term trend of SST variabilities, on the regional scales, affected by the coastal upwelling, may be moderated due to the possible dominance of any other oceanic-climatic phenomena on coastal water dynamics. This ambiguity can largely be related to the resolution of the investigated SST data.

Zonal and meridional wind speed components were extracted from the ECMWF's ERA-5 re-analysis² for the period spanning from 1979 to 2020, for a total of 42 years with monthly time steps (Hersbach *et al.*, 2020). To enhance the diagnostic capabilities of the initial results, the initial $25 \times 25 \text{ km}^2$ winds were interpolated onto a $5 \times 5 \text{ km}^2$ gridded data set, aligning with

¹ https://resources.marine.copernicus.eu/product-detail/SST_GLO_SST_L4_NRT_OBSERVATIONS_010_001/

² <https://cds.climate.copernicus.eu/cdsapp#!/dataset/reanalysis-era5-single-levels>

the spatial resolutions of the OSTIA data products. Next, the wind speed components were retrieved, and the wind stress components were computed using the quadratic bulk aerodynamic formulation outlined in Hellerman and Rosenstein (1983). The longitudinal (Q_x) and latitudinal (Q_y) components of the Ekman transport were, then, calculated (Schwing *et al.*, 1996; Cropper *et al.*, 2014). Based on the Ekman transport components, the Coastal Upwelling Index (*CUI*) was estimated with the following equation (Gomez-Gesteira *et al.*, 2006):

$$CUI = -Q_x \sin\left(\theta - \frac{\pi}{2}\right) + Q_y \cos\left(\theta - \frac{\pi}{2}\right) \quad (1)$$

where q is the angle of the oceanward unit vector that is perpendicular to the mean shoreline position. In fact, the *CUI* detects coastal upwelling occurrence considering the Ekman transport intensity (Q_x , Q_y) and its direction towards the shoreline orientation. A positive (or negative) value of *CUI* implies that the Ekman transport has an oceanward (or landward) component, and the value close to zero implies that the dominated vector of the Ekman transport is parallel to the coastline. To estimate the wind-driven coastal upwelling system in comparison with the SST data variations, the 42-year mean annual cycle (monthly climatology) of *CUI* is linearly interpolated in each of the five-kilometre intervals along the Makran coasts (57°-67° E). Furthermore, given the expected influence of q on the spatial distribution of coastal upwelling intensity, a line fitting analysis was conducted within each of the five-kilometre intervals to match the resolution of the interpolated wind data. This analysis was performed on a full-resolution extraction of the Global Self-consistent, Hierarchical, High-resolution Shoreline³ database (Wessel and Smith, 1996). For each of the five-kilometre longitudinal sections, the wind speed components were determined at the data grid-point nearest to the shoreline location of that section. As a result, positive and negative values of the *CUI* correspond to favourable coastal upwelling and downwelling conditions, respectively, with higher positive or negative values indicating more intense occurrences.

Furthermore, the monthly climatology of temperature profiles, from the surface to a depth of 100 m, was estimated by following the approach suggested by Morvan *et al.* (2020). This climatology covers the period from 1993 to 2019, and is based on weekly ARMOR3D⁴ multi-year reprocessed data (Guinehut *et al.*, 2012; Mulet *et al.*, 2012). The ARMOR3D product is a composite data set that combines both satellite and in-situ data sources. Similarly to the *CUI*, the temperature profiles were determined at the data grid-point closest to the shoreline location of each section.

A 20-year data set (2000-2019) containing geostrophic and Ekman components of sea surface current data, with a spatial resolution of 25 km, was also acquired from the Geostrophic and Ekman Current Observatory (GEKCO). The GEKCO model, developed by Sudre *et al.* (2013), utilises remote-sensing altimeter and scatterometer data sets to provide both geostrophic and Ekman currents, and its outputs are available from the Laboratory of Space Geophysical and Oceanographic Studies⁵, upon request. By assessing the intensity of the Ekman current component, in comparison with the geostrophic current component, we aim to improve the detection of temporal and spatial changes in the potential wind-driven coastal upwelling system along the Makran coasts.

³ <https://www.ngdc.noaa.gov/mgg/shorelines/>

⁴ https://resources.marine.copernicus.eu/product-detail/MULTIOBS_GLO_PHY_TSUV_3D_MYNRT_015_012/

⁵ <https://www.legos.omp.eu/en/data/>

3. Results and discussion

3.1. The SST Trend

Since the coastal upwelling mechanism is associated with cold deep waters moving up to the sea surface and with the subsequent sea breezes, the frequent and severe occurrences of coastal upwelling are expected to moderate the long-term SST trend of coastal waters (Bakun, 1990). Hence, many studies use the trend analysis of long-term SST records in coastal waters as a diagnostic tool for detecting coastal upwelling occurrence and intensity. Fig. 2 shows the SST trend of the last 14 years in the northern Arabian Sea.

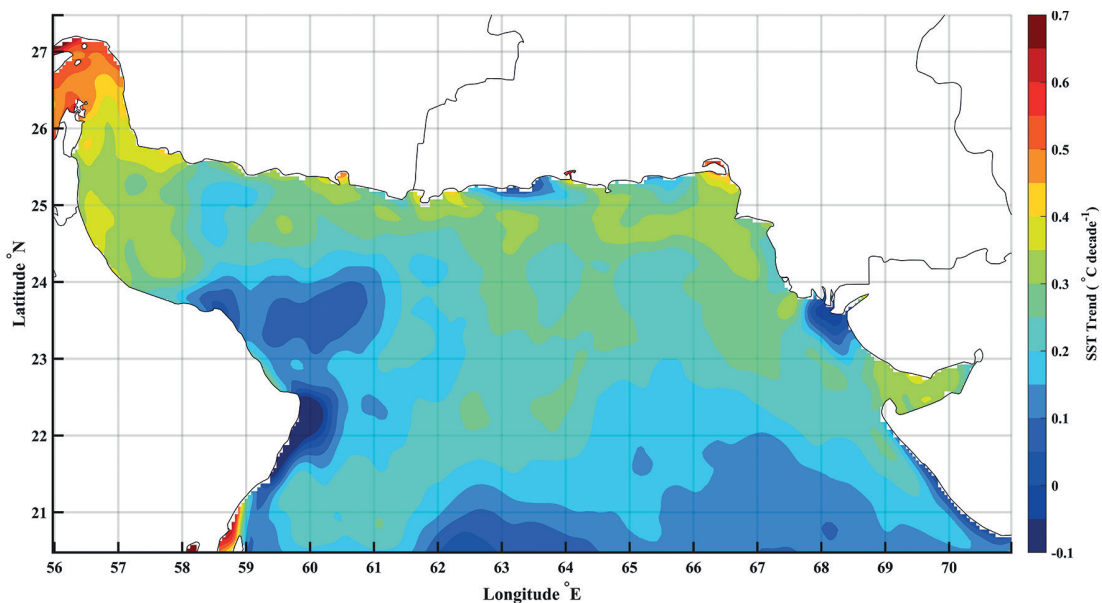


Fig. 2 - The SST trend based on 14 years of OSTIA data product.

As Fig. 2 demonstrates, the upwelling areas, in the west and east of the Arabian Sea, identified by previous studies (Vic *et al.*, 2017; Jayaram and Kumar, 2018), are characterised by a reduced SST trend. Also, the north-western part of the Arabian Sea, approximately 23.5° N and 68° E, is close to the high wind energy zone in the southern part of Pakistan and the Indus River delta (Nayyar and Zaigham, 2013; Mahar and Zaigham, 2015), where water discharge from a large river reduces the SST in the coastal area (Jaiganesh *et al.*, 2021). The two other noteworthy points are located along the eastern Makran coasts, approximately 25° N, along 62°-64° E and 65°-66° E. These reductions in the SST trend are rather similar to other well-known coastal upwelling systems in the eastern and western Arabian Sea. In addition, based on data resolution, the trend analysis shows that SST variability and the severity of cooling mechanisms is not uniform along the Makran coasts. However, if coastal upwelling is assumed to be one of the coastal water cooling mechanisms, due to the fact that the wind speed patterns are not significantly variable across this relatively small area (Anoop *et al.*, 2020; Aboobacker *et al.*, 2021), then, the second factor, the coastline angle (q), will be expected to be responsible for this variable SST trend along the Makran coasts.

In summary, these findings suggest that wind patterns over Makran, in conjunction with the specific geometry of certain coastal sections, favour the occurrence of upwelling. This, in turn, leads to a significant decrease in SST, particularly along the sections around 63°-64° E and 65°-66° E. Worthy of note are previous studies (Khan *et al.*, 2004; Rana *et al.*, 2014) that observed an increasing SST trend throughout all seasons in the northern Arabian Sea and its coastal zones. Therefore, the primary hypothesis of this study is that coastal upwelling occurs more significantly in western parts of the Makran coasts than in eastern parts, in contrast to the increasing SST trend and long-term warming of coastal waters.

The SST trend analysis implies that the existence of a coastal upwelling system along the Makran coasts is not far from what is expected. However, variabilities in sea surface parameters are related to all dynamic factors of a basin. It should be noted that, as already proven by several studies, the surface mesoscale, as well as submesoscale eddies, impact the circulation system of the northern Arabian Sea (Eshghi *et al.*, 2022; Font *et al.*, 2022; Smitha *et al.*, 2022). As demonstrated by L'Hegaret *et al.* (2015), the outflow from the Persian Gulf to the Gulf of Oman presents several offshore ejection sites and a complex recirculation, depending on the mesoscale eddies. The outflow path in the Makran coastal waters can be, up to approximately 59° E, parallel to the Makran coasts before it changes to the southern parts of the Gulf of Oman (oceanwards). Furthermore, submesoscale eddies can be the results of local coastal upwelling (Morvan *et al.*, 2020). In any case, it is important to understand the extent to which these factors overshadow the dynamics of coastal currents.

3.2. CUI evaluation

Fig. 3 displays the 42-year mean annual cycle of the CUI. The top panel of Fig. 3 illustrates the q values, estimated in this study, for each longitudinal section; the bottom panel shows the 42-year monthly climatology of the CUI. From an initial examination, the coastal upwelling exhibits significant intensity, around 63°-64° E and 65°-66° E.

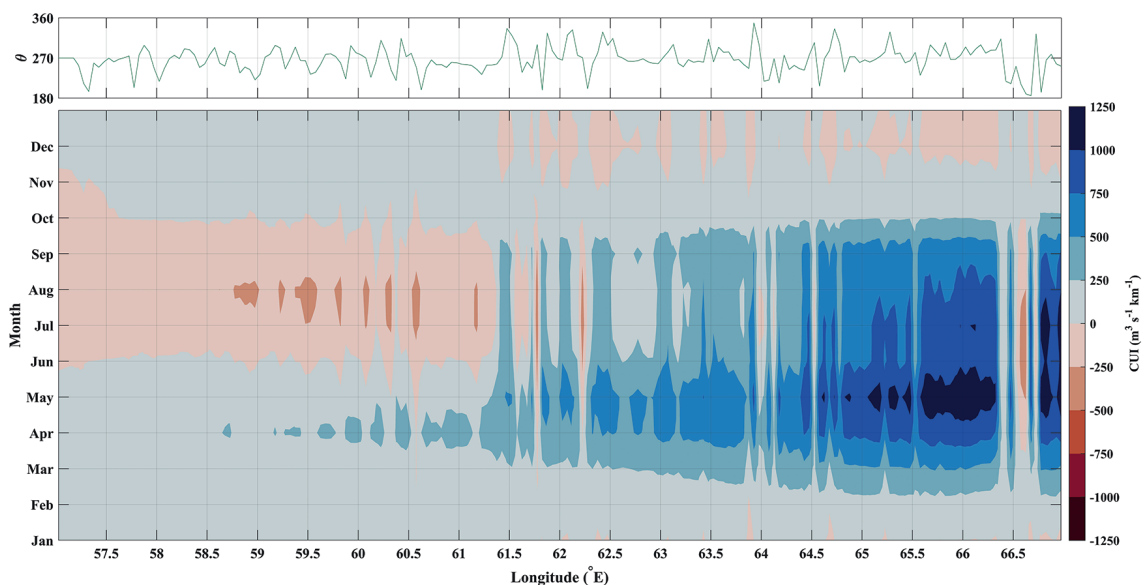


Fig. 3 - The 42-year mean annual cycles of CUI and the q values.

Based on Fig. 3, the most intense coastal upwellings are detected in May. There are slight local coastal upwelling events, around 58°-61° E. The *CUI* also shows that there is a very slight downwelling around 57°-61° E. Due to the more exact q values for the calculation of the *CUI* being considered in this study, the effect of the smaller scale variabilities is also highlighted in Figs. 2 and 3. Consequently, this demonstrates that q can be very important in coastal upwelling intensity. For example, as shown in Fig. 2, coastal upwelling at 64°-65° E and, also, at 66°-67° E is not expected to be significant, as no significantly decreasing SST trend has been found in this location. Conversely, the intensity of the coastal upwelling system along 62°-64° E should be larger than that along 65°-66° E, according to Fig. 2, whereas Fig. 3 proves that the *CUI* is stronger in the 65°-66° E range.

3.3. Coastal temperature profile

Fig. 4 shows the mean annual cycle of temperature profile along the Makran coasts, from the surface to the depth of 100 m. The vertical temperature gradient in the first three months (cold season) is not intense. However, from April the surface layers become warmer. The warming is modified in May by the vertical transfer of the waters to the surface, as clearly shown by the 62°-66° E area, indicating the occurrence of a significant coastal upwelling pattern, which continues from May until December, while its intensity decreases.

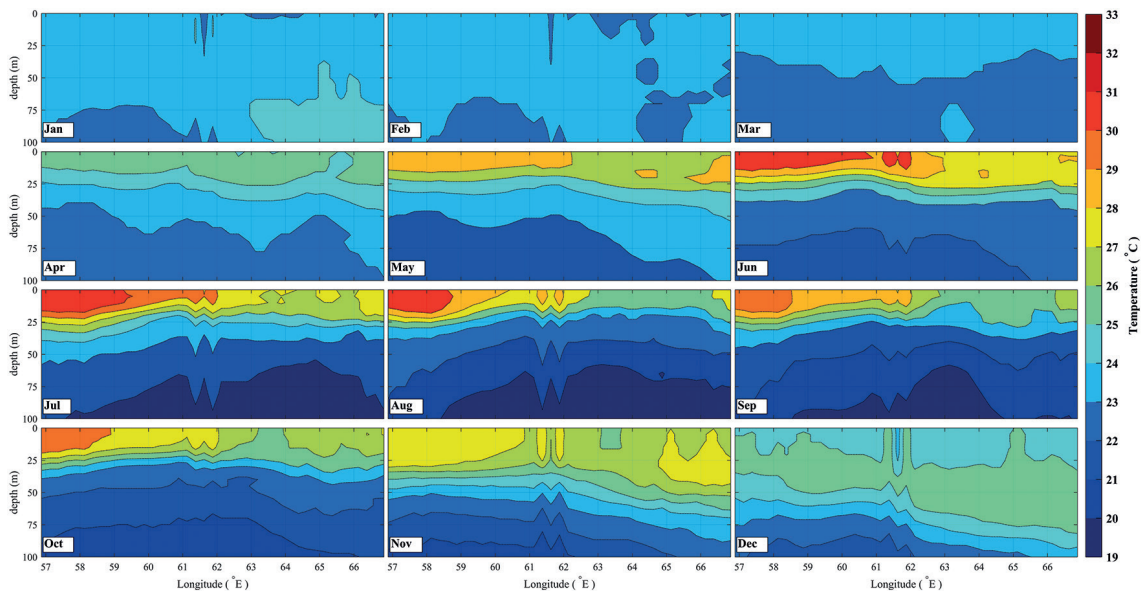


Fig. 4 - The 27-year mean vertical temperature along the Makran coasts based on ARMOR3D re-analysis data.

Fig. 4, obtained using 25-kilometre resolution data, is in very good agreement with Fig. 3. Likewise, from June to September (summer season), a warm zone that exists on the surface of the coastal waters of western Makran, even though all the coasts of Makran are located at a relatively constant latitude, does not involve the eastern coasts. This shows that the coastal upwelling system prevents severe warming of coastal waters in summer along the eastern Makran coasts. However, the temporal changes of this system are similar to the Indian summer monsoons, and the monsoon seasonal cycle also affects the SST changes (Das *et al.*, 2013).

3.4. Coastal upwelling, SST, and monsoon

Vinayachandran (2004) stated that the duration of the upwelling off the coast of Somalia, and its lateral advection, appears to be a significant parameter on which the summer cooling depends. Other previous studies have mentioned the upwelling effect on the summer cooling of the Arabian Sea, but none of them referred to the northern part of the Arabian Sea, specifically to the coastal upwelling system along the Makran coasts (McCreary and Kundu, 1989; Shankar *et al.*, 2002; Varela *et al.*, 2018). To explore this uncertainty further, the monsoon index was extracted following the methodology of Wang *et al.* (2001). Next, a correlation analysis was conducted between the time series of the summer monsoon index and sea surface SST. Additionally, another correlation analysis was performed between the monsoon index and the *CUI* along each of the five-kilometre longitudinal sections along the Makran coasts. These analyses were conducted simultaneously, within corresponding time intervals, from the monthly time series data.

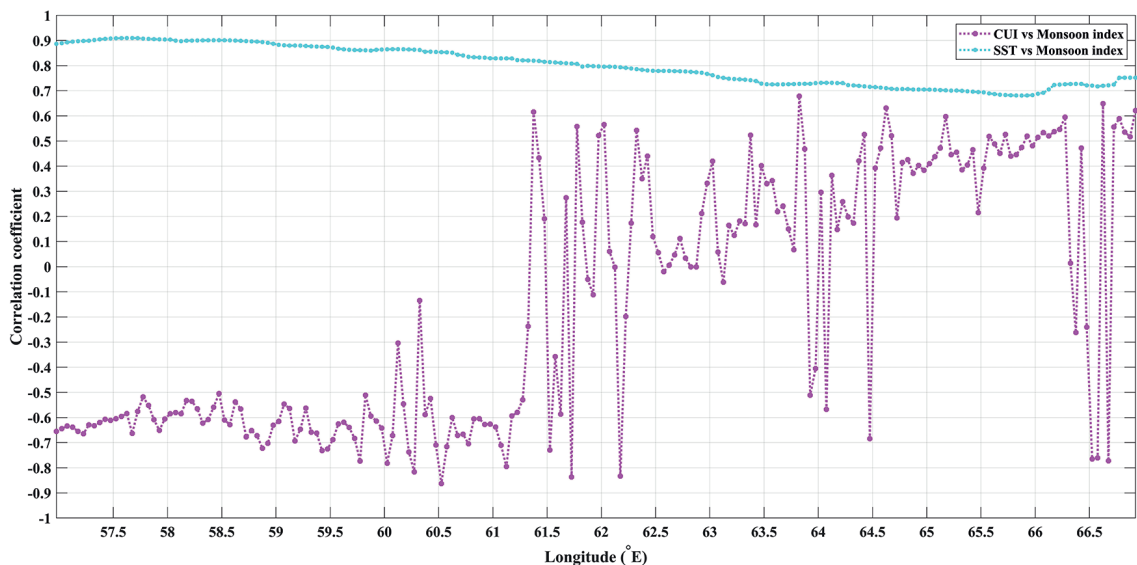


Fig. 5 - The correlation coefficient for an analysis between the *CUI* and monsoon index, and for the analysis between the SST and monsoon index.

Fig. 5 reveals a noteworthy correlation between SST variations along the Makran coasts and the summer monsoon. As expected, the monsoon index exhibits a similar variation to temperature, with two peaks during the warm months. However, this correlation gradually diminishes from west to east. This could indicate that, in the eastern Makran, a factor, such as coastal upwelling, slightly reduces the effect of the summer monsoon on the SST variations. The *CUI* variations show less correlation with the monsoon in several longitudinal sections. Therefore, the *CUI* changes can be acknowledged as being correlated with SST changes, regardless of the seasonal variability component. For further investigation, the typical seasonal cycle was removed from the *CUI* and SST time series, and a correlation analysis was performed between them. Fig. 6 shows a correlation coefficient between the deseasonalised SST and *CUI* time series for each of the five-kilometre longitudinal sections. According to these results, the deseasonalised SST

variations are more strongly correlated with the *CUI* along the eastern Makran coasts, especially at the sections with higher *CUI* peaks, shown in Fig. 3. According to Fig. 6, deseasonalised SST variations along the eastern Makran coasts are more strongly, and inversely, correlated with the *CUI* in comparison with the other area.

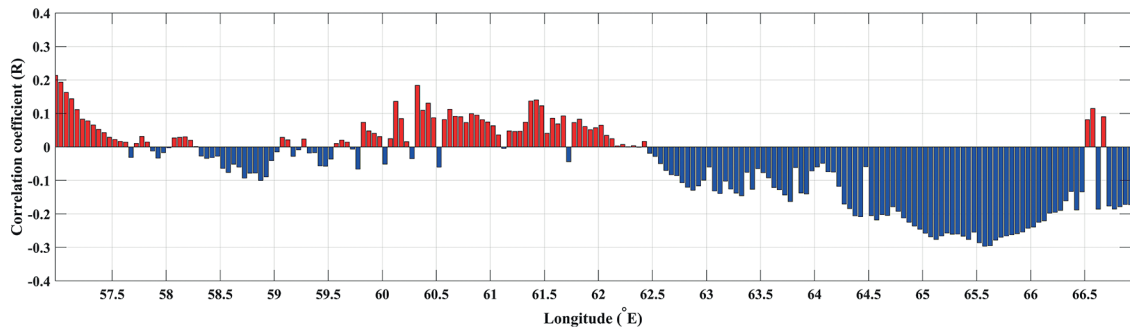


Fig. 6 - The correlation coefficient between deseasonalised SST and *CUI* time series.

Inverse correlation implies that an increase in *CUI* coincides with a decrease in the SST value. The strongest correlation coefficient is found in the region between 65° and 66° E, where the most intense coastal upwelling events are evident, as depicted in Fig. 3. Conversely, in areas where significant coastal upwelling patterns were not anticipated (Figs. 4 and 5), or where slight downwelling events were possible (Fig. 3), the correlation coefficient tends to be positive or close to zero, indicating a lack of statistically significant influence of coastal upwelling on SST variability in such areas.

In addition, the results in Fig. 6 show that a significant signal of coastal upwelling along the eastern Makran coasts is wind-driven, despite the other factors that could have a significant effect on the coastal water dynamics. In general, all the results presented in Figs. 2 to 6 of this study (each of which is obtained from different data and methods) testify to the existence of a significant seasonal upwelling system along the eastern Makran coasts, peaking and coinciding with the summer monsoon in May, and lasting until mid-autumn.

3.5. Sea surface current

Despite the alignment of the results in the spatiotemporal SST and *CUI* patterns, changing along the eastern Makran coasts, a matter of controversy concerns whether wind-driven currents in the coastal areas are affected by other sea surface current components. In this study, to address this issue, the climatology of two main sea surface current components were evaluated using GECKO2 data from 2000 to 2019. Figs. 7 and 8 show the 20-year mean annual cycles of the sea surface Ekman current component and geostrophic current component, respectively, the sum of which can be a good estimate of the total sea surface current.

According to Fig. 7, the Ekman current component is dominant in the north-eastern Arabian Sea. In addition, based on Fig. 8, the geostrophic current component prevails in the Gulf of Oman with a local cyclonic gyre (mesoscale eddy) that peaks in winter along the western Makran coasts. However, this gyre naturally reduces the probability of wind-driven coastal upwelling occurrences and can increase the likelihood of eddy-induced upwelling. Nevertheless, since there is no evidence indicating a significant temperature decrease along the western Makran

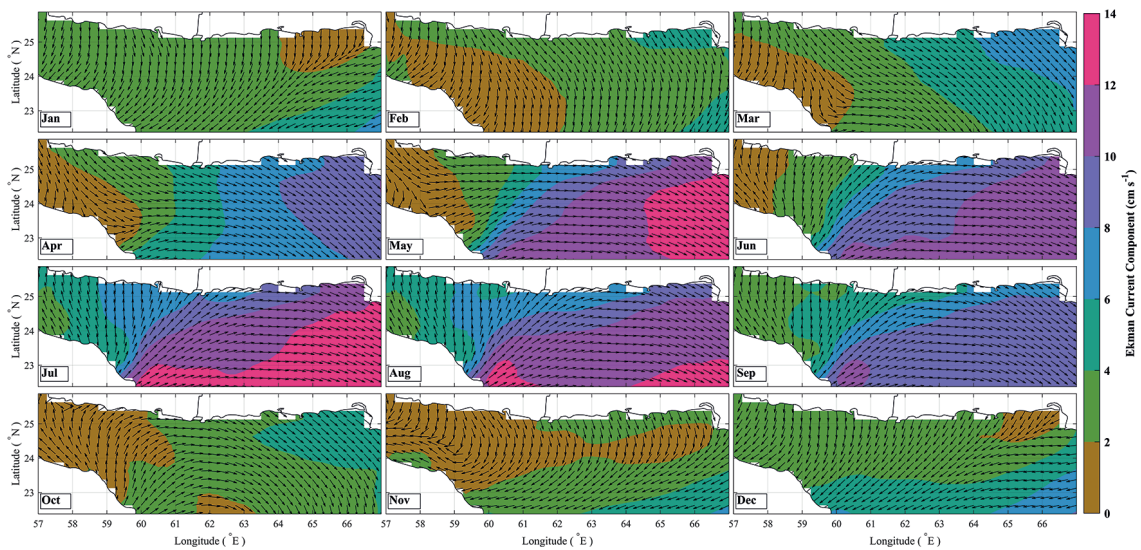


Fig. 7 - The 20-year (2000-2019) mean annual cycle of the sea surface Ekman current component.

coasts, this aspect is not explored any further in this study. Worthy of mention is that, as described by Ayouche *et al.* (2021), the cyclonic gyre initially forms at the mouth of the Gulf of Oman, near the western Makran coasts, and, then, gradually drifts south-eastwards from early to mid-June. Then, it remains stationary at the same location and elongates until mid-August. Fig. 8 also highlights a prominent mesoscale eddy pattern between longitudes 62° and 65° E along the Makran coasts during June. In addition, it is demonstrated that the geostrophic current component values during April-June are very low along the eastern Makran coasts. This indicates that the intense wind-driven coastal upwelling activities overcome the surface eddy structure. There are also less decreased values of the geostrophic current component in other months, especially along 62°-64° E and 65°-66° E.

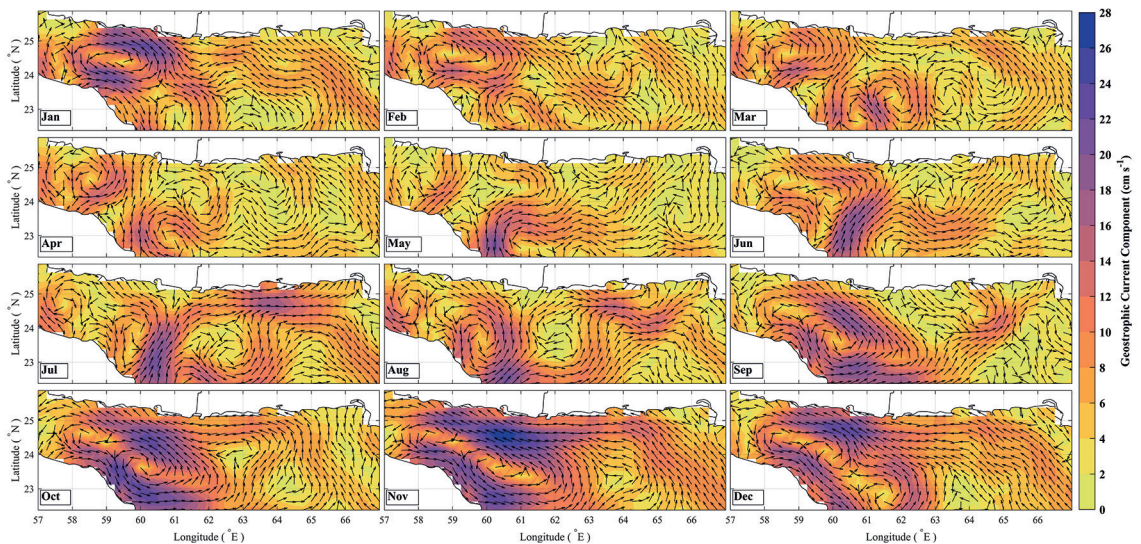


Fig. 8 - The 20-year (2000-2019) mean annual cycle of the sea surface geostrophic current component.

During June, along the eastern Makran coasts, however, the Ekman current component continues to dominate, suggesting favourable conditions for upwelling (Fig. 7). At the same time, the geostrophic component, influenced by sea level changes along the Makran coasts (Fig. 8), is expected to form, and potentially reduce, the coastal upwelling intensity in June. By comparing Figs. 3, 7, and 8, the coastal upwelling system is understandably significant and intense along the eastern Makran coasts only when the magnitude of the geostrophic component current is not more than 4 cm/s, and the Ekman component prevails in the northern Arabian Sea. In other months, the interaction of these two components is such that the greater the Ekman component, compared to the geostrophic component in the northern Arabian Sea, the more intense the coastal upwelling along the eastern Makran coasts.

4. Conclusions

The existence of a coastal upwelling system along the Makran coasts, and its possible spatiotemporal variabilities, have been investigated in this study. Initially, the trend analysis of the high-resolution satellite SST data shows a relative decrease in temperature trends along the Makran coasts, which could represent an upwelling system similar to the other well-known coastal upwelling system in the Arabian Sea. However, it is important to note that this decreasing trend is not uniform, thus, indicates the presence of smaller-scale instabilities in the Makran waters. Accordingly, the present study demonstrates the importance of investigating the smaller scale instabilities in order to better detect regional sea surface dynamics and recognise the effects of climate change. To evaluate the variabilities of coastal upwelling on smaller scales, the *CUI* was computed by interpolating coastline data in each longitudinal interval of 5 km along the Makran coasts, and by reducing wind stress to this scale. Then, the vertical temperature structure was evaluated and, finally, the spatiotemporal patterns of sea surface current components were considered across the northern Arabian Sea and the Gulf of Oman. The main results obtained in the study are summarised as follows.

The wind regimes in the northern Arabian Sea from late winter to late summer (from early March to mid-September) are favourable to the presence of an upwelling system along the Makran coasts, with the Ekman transport reaching $500 \text{ m}^3\text{s}^{-1}\text{km}^{-1}$, and being directed offshore. The mean horizontal Ekman transport value, calculated for the coastal water segment closest to the shoreline, has been evaluated to induce coastal upwelling, as demonstrated in prior studies conducted in different basins (Alvarez *et al.*, 2011; Barzandeh *et al.*, 2018; Sousa *et al.*, 2020). However, along the eastern Makran coasts, from early April to mid-August, when the oceanward Ekman transport mean at the coastal water segment closest to the shoreline reaches more than $750 \text{ m}^3\text{s}^{-1}\text{km}^{-1}$, the vertical temperature structure changes and, clearly, some signs of thermocline, appear starting from April. When the Ekman transport mean peaks to more than $1,000 \text{ m}^3\text{s}^{-1}\text{km}^{-1}$ in April-May, the mean temperature profile shows the vertical transport of cold waters to the upper layers.

All the results that were obtained using the new long-term data only show the coastal upwelling system for the eastern Makran coasts and, also, indicate that in the western Makran coasts, i.e. along the northern shoreline of the Gulf of Oman (Iranian coasts), there is no significant coastal upwelling pattern. This contrasts with some previous studies that were referred to in the introduction to the present study. Although previous studies did not make significant use of big data analyses to identify the coastal upwelling system along the Iranian coasts, they mentioned the possibility of doing so. However, the results of this study clearly show that there is no coastal

upwelling along the Iranian coasts, due to the decrease of wind-driven surface currents and the predominance of geostrophic flows that imply the mesoscale eddy structure in the Gulf of Oman. The mesoscale eddies, in the northern Arabian Sea, limit the Makran coastal upwelling system in summer, and, despite the strong wind regime and the monsoon currents, eddies could also limit the coastal upwelling system and cause a reduction of its intensity in summer. However, the interaction of winds and eddies can lead to mild coastal upwelling patterns by September. The deseasonalised coastal upwelling signals, and their interactions with SST variabilities on the eastern Makran coasts, specifically between 65° and 66° E, show that the seasonal Makran systems are wind-driven. In subregions, such as 63°-64° E, where the wind-driven coastal upwelling intensity is a little milder but the decreasing SST trend is more pronounced, other factors (such as eddies) can be recognised as the co-drivers of the coastal upwelling system along the eastern Makran coasts. Conversely, the coastal upwelling mechanism collapses due to spatial changes in the shoreline angle. Such changes also occur approximately at longitudes of 64.5° or 66.5° E, and provide evidence of downwelling, instead of the coastal upwelling pattern, leading to a positive SST change rate along the Makran coasts. But even these small changes, as shown by results of the trend analysis of high-resolution SST data and the spatiotemporal distribution of *CUI*, affect the coastal water warming process and, consequently, the vertical distribution of ocean properties.

Regionally, the present study demonstrated that the hypothesis of a significant effect of wind-driven smaller-scale instabilities, on long-term changes in coastal waters, is valid only for the eastern Makran coasts and is inconceivable in the western Makran coasts. In addition, by observing the results obtained in this study, the cooling process in Makran coastal waters can be assumed to be mainly related to wind-driven currents and coastal upwelling, and, despite the mesoscale eddy activity in the Gulf of Oman and the northern Arabian Sea, the eddies could influence temperature variability only in offshore areas.

REFERENCES

- Aboobacker V.M., Vethamony P. and Rashmi R.; 2011: "*Shamal*" swells in the Arabian Sea and their influence along the west coast of India. *Geophys. Res. Lett.*, 38, 1-7, doi: 10.1029/2010GL045736.
- Aboobacker V.M., Shanas P.R., Al-Ansari Ebrahim M.A.S., Sanil Kumar V. and Vethamony P.; 2021: *The maxima in northerly wind speeds and wave heights over the Arabian Sea, the Arabian/Persian Gulf and the Red Sea derived from 40 years of ERA5 data.* *Clim. Dyn.*, 56, 1037-1052, doi: 10.1007/s00382-020-05518-6.
- Akhvani M., Chegini V. and Bidokhti A.A.; 2015: *An appraisal of the power density of current profile in the Persian Gulf and the Gulf of Oman using numerical simulation.* *Renew. Energy*, 74, 307-317.
- Al-Azri A.R., Piontkovski S.A., Al-Hashmi K.A., Goes J.I. and do Gomes H.R.; 2010: *Chlorophyll a as a measure of seasonal coupling between phytoplankton and the monsoon periods in the Gulf of Oman.* *Aquat. Ecol.*, 44, 449-461, doi: 10.1007/s10452-009-9303-2.
- Alvarez I., Gomez-Gesteira M., deCastro M., Lorenzo M.N., Crespo A.J.C. and Dias J.M.; 2011: *Comparative analysis of upwelling influence between the western and northern coast of the Iberian Peninsula.* *Cont. Shelf Res.*, 31, 388-399, doi: 10.1016/j.csr.2010.07.009.
- Anoop T.R., Shanas P.R., Aboobacker V.M., Kumar V.S., Nair L.S., Prasad R. and Reji S.; 2020: *On the generation and propagation of Makran swells in the Arabian Sea.* *Int. J. Clim.*, 40, 585-593, doi: 10.1002/joc.6192.
- Ayouche A., De Marez C., Morvan M., L'Hegaret P., Carton X., Le Vu B. and Stegner A.; 2021: *Structure and dynamics of the Ras al Hadd oceanic dipole in the Arabian Sea.* *Oceans*, 2, 105-125, doi: 10.3390/oceans2010007.
- Bakun A.; 1990: *Global climate change and intensification of coastal ocean upwelling.* *Sci.*, 247, 198-201.
- Banse K.; 1997: *Irregular flow of Persian (Arabian) Gulf water to the Arabian Sea.* *J. Mar. Res.*, 55, 1049-1067.
- Barzandeh A., Eshghi N., Hosseinibalam F. and Hassanzadeh S.; 2018: *Wind-driven coastal upwelling along the northern shoreline of the Persian Gulf.* *Boll. Geof. Teor. Appl.*, 59, 301-312, doi: 10.4430/bgta0235.

- Chaichitehrani N. and Allahdadi M.N.; 2018: *Overview of wind climatology for the Gulf of Oman and the northern Arabian Sea*. Am. J. Fluid Dyn., 8, 1-9.
- Chollett I., Müller-Karger F.E., Heron S.F., Skirving W. and Mumby P.J.; 2012: *Seasonal and spatial heterogeneity of recent sea surface temperature trends in the Caribbean Sea and southeast Gulf of Mexico*. Mar. Pollut. Bull., 64, 956-965.
- Cropper T.E., Hanna E. and Bigg G.R.; 2014: *Spatial and temporal seasonal trends in coastal upwelling off northwest Africa, 1981-2012*. Deep Sea Res. Part I, 86, 94-111.
- Das S.K., Deb S.K., Kishtawal C.M. and Pal P.K.; 2013: *Seasonal prediction of Indian summer monsoon: sensitivity to persistent SST*. J. Earth Syst. Sci., 122, 1183-1193, doi: 10.1007/s12040-013-0351-6.
- Eshghi N., Barzandeh A., Hosseinibalam F. and Hassanzadeh S.; 2020: *Investigating dynamic and static aspects of regional sea level changes in the north-western Indian Ocean*. Boll. Geof. Teor. Appl., 61, 249-270, doi: 104430/bgta0298.
- Eshghi N., Mohammadian A. and Mahdizadeh M.M.; 2022: *The effect of Ekman and geostrophic surface current on the distribution of SST variability over the Persian Gulf*. Arabian J. Geosci., 15, 1-12.
- Findlater J.: 1969: *A major low-level air current near the Indian Ocean during the northern summer*. Q. J. R. Meteorolog. Soc., 95, 362-380.
- Font E., Queste B.Y. and Swart S.; 2022: *Seasonal to intraseasonal variability of the upper ocean mixed layer in the Gulf of Oman*. J. Geophys. Res.: Oceans, 127, e2021JC018045, 42 pp., doi: 10.1029/2021JC018045.
- Fritz H.M., Blount C.D., Albusaidi F.B. and Al-Harthy A.H.M.; 2010: *Cyclone Gonu storm surge in Oman*. Estuarine, Coastal and Shelf Sci., 86, 102-106, doi: 10.1016/j.ecss.2009.10.019.
- Ghaemi Bajestani H., Rahbani M. and Sharbati S.; 2018: *Investigating the potentiality of upwelling in the coastal area of Jask Headland*. Hydrophys., 4, 69-84.
- Glejin J., Kumar V.S., Nair T.N.B., Singh J. and Mehra P.; 2013: *Observational evidence of summer Shamal swells along the west coast of India*. J. Atmos. Oceanic Technol., 30, 379-388, doi: 10.1175/JTECH-D-12-00059.1.
- Gomez-Gesteira M., Moreira C., Alvarez I. and deCastro M.; 2006: *Ekman transport along the Galician coast (northwest Spain) calculated from forecasted winds*. J. Geophys. Res., 111, C10005, 12 pp., doi: 10.1029/2005JC003331.
- Good S., Fiedler E., Mao C., Martin M.J., Maycock A., Reid R., Roberts-Jones J., Searle T., Waters J., While J. and Worsfold M.; 2020: *The current configuration of the OSTIA system for operational production of foundation sea surface temperature and ice concentration analyses*. Remote Sens., 12, 720, 20 pp., doi: 10.3390/rs12040720.
- Guinehut S., Dhomps A.-L., Larnicol G. and Le Traon P.-Y.; 2012: *High resolution 3-D temperature and salinity fields derived from in situ and satellite observations*. Ocean Sci., 8, 845-857, doi: 10.5194/os-8-845-2012.
- Hassanzadeh S. and Hosseinibalam F.; 2020: *Mean sea level variability of the Oman Sea and its response to monsoon and the North Atlantic oscillation index from tide gauge measurements*. J. Agric. Mar. Sci., 26, 37-46.
- Hellerman S. and Rosenstein M.; 1983: *Normal monthly wind stress over the world ocean with error estimates*. J. Phys. Oceanogr., 13, 1093-1104.
- Hersbach H., Bell B., Berrisford P., Hirahara S., Horányi A., Muñoz-Sabater J., Nicolas J., Peubey C., Radu R., Schepers D., Simmons A., Soci C., Abdalla S., Abellan X., Balsamo G., Bechtold P., Biavati G., Bidlot J., Bonavita M., De Chiara G., Dahlgren P., Dee D., Diamantakis M., Dragani R., Flemming J., Forbes R., Fuentes M., Geer A., Haimberger L., Healy S., Hogan R.J., Hólm E., Janisková M., Keeley S., Laloyaux P., Lopez P., Lupu C., Radnoti G., de Rosnay P., Rozum I., Vamborg F., Villaume S. and Thépaut J.-N.; 2020: *The ERA5 global reanalysis*. Q. J. R. Meteorolog. Soc., 146, 1999-2049, doi: 10.1002/qj.3803.
- Jaiganesh S., Sarangi R.K. and Shukla S.; 2021: *Satellite-based observation of ocean productivity in southeast Arabian Sea using chlorophyll, sea surface temperature and wind datasets*. J. Earth Syst. Sci., 130, 1-13.
- Jayaram C. and Kumar P.D.; 2018: *Spatio-temporal variability of upwelling along the southwest coast of India based on satellite observations*. Cont. Shelf Res., 156, 33-42.
- Johns W.E., Jacobs G.A., Kindle J.C., Murray S.P. and Carron M.; 1999: *Arabian marginal seas and gulfs*. In: Proc. Workshop, Naval Research Laboratory, Oceanography Division, Stennis Space Center, MS, USA, Report NRL/PP/7330-00-0024, 59 pp.
- Kämpf J. and Chapman P.; 2016: *The functioning of coastal upwelling systems*. In: Upwelling systems of the world, Kämpf J. and Chapman P. (eds), Springer International Publishing, Cham, Switzerland, pp. 31-65, doi: 10.1007/978-3-319-42524-5_2.

- Kaul N., Rosenberger A. and Villinger H.; 2000: *Comparison of measured and BSR-derived heat flow values, Makran accretionary prism, Pakistan*. Mar. Geol., 164, 37-51.
- Khan T.M.A., Quadir D.A., Murty T.S. and Sarker M.A.; 2004: *Seasonal and interannual sea surface temperature variability in the coastal cities of Arabian Sea and Bay of Bengal*. Nat. Hazards, 31, 549-560, doi: 10.1023/B:NHAZ.0000023367.66009.1d.
- L'Hégaret P., Lacour L., Carton X., Rouillet G., Baraille R. and Corréard S.; 2013: *A seasonal dipolar eddy near Ras Al Hamra (Sea of Oman)*. Ocean Dyn., 63, 633-659, doi: 10.1007/s10236-013-0616-2.
- L'Hégaret P., Duarte R., Carton X., Vic C., Ciani D., Baraille R. and Corréard S.; 2015: *Mesoscale variability in the Arabian Sea from HYCOM model results and observations: impact on the Persian Gulf water path*. Ocean Sci., 11, 667-693, doi: 10.5194/os-11-667-2015.
- Lehmann A., Myrberg K. and Höfllich K.; 2012: *A statistical approach to coastal upwelling in the Baltic Sea based on the analysis of satellite data for 1990-2009*. Oceanolog., 54, 369-393.
- Lu X., Huang C., Chen F., Zhang S., Lao Q., Chen C., Wu J., Jin G. and Zhu Q.; 2021: *Carbon and nitrogen isotopic compositions of particulate organic matter in the upwelling zone off the east coast of Hainan Island, China*. Mar. Pollut. Bull., 167, 112349, 8 pp., doi: 10.1016/j.marpolbul.2021.112349.
- Mahar G.A. and Zaigham N.A.; 2015: *Examining spatio-temporal change detection in the Indus River Delta with the help of satellite data*. Arabian J. Sci. Eng., 40, 1933-1946.
- McCreary J.P. and Kundu P.K.; 1989: *A numerical investigation of sea surface temperature variability in the Arabian Sea*. J. Geophys.: Oceans, 94, 16097-16114.
- Moradi M.; 2016: *Identification of upwelling areas in the Oman Sea using satellite data*. In: Abstract 41st COSPAR Scientific Assembly, Istanbul, Turkey, A2.2-3-16, 14 pp.
- Morvan M., Carton X., Corréard S. and Baraille R.; 2020: *Submesoscale dynamics in the Gulf of Aden and the Gulf of Oman*. Fluids, 5, 146, 19 pp., doi: 10.3390/fluids5030146.
- Mulet S., Rio M.-H., Mignot A., Guinehut S. and Morrow R.; 2012: *A new estimate of the global 3D geostrophic ocean circulation based on satellite data and in-situ measurements*. Deep Sea Res. Part II, 77, 70-81, doi: 10.1016/j.dsr2.2012.04.012.
- Muraleedharan P., Mohankumar K. and Sivakumar K.; 2013: *A study on the characteristics of temperature inversions in active and break phases of Indian summer monsoon*. J. Atm. Sol. Terr. Phys., 93, 11-20.
- Murtugudde R., Seager R. and Thoppil P.; 2007: *Arabian Sea response to monsoon variations*. Paleoceanogr., 22, PA4217, 17 pp., doi: 10.1029/2007PA001467.
- Nayyar Z.A. and Zaigham N.A.; 2013: *Assessment of wind potential in southeastern part of Pakistan along coastal belt of Arabian sea*. Arabian J. Sci. Eng., 38, 1917-1927.
- Pond S. and Pickard G.L.; 1983: *Introductory dynamical oceanography, 2 ed.* Butterworth-Heinemann Ltd, Oxford, UK, 329 pp.
- Pous S., Carton X. and Lazure P.; 2004: *Hydrology and circulation in the Strait of Hormuz and the Gulf of Oman - Results from the GOGP99 Experiment: 2. Gulf of Oman*. J. Geophys. Res.: Oceans, 109, C12, 36 pp., doi: 10.1029/2003JC002146.
- Prasad T., Ikeda M. and Kumar S.P.; 2001: *Seasonal spreading of the Persian Gulf water mass in the Arabian Sea*. J. Geophys. Res.: Oceans, 106, 17059-17071.
- Pratik K., Parekh A., Karmakar A., Chowdary J.S. and Gnanaseelan C.; 2019: *Recent changes in the summer monsoon circulation and their impact on dynamics and thermodynamics of the Arabian Sea*. Theor. Appl. Climatol., 136, 321-331, doi: 10.1007/s00704-018-2493-6.
- Rana A., Zaman Q., Afzal M. and Haroon M.A.; 2014: *Characteristics of sea surface temperature of the Arabian Sea coast of Pakistan and impact of tropical cyclones on SST*. Pakistan J. Meteorol., 11, 61-70.
- Reul A., Rodríguez V., Jiménez-Gómez F., Blanco J.M., Bautista B., Sarhan T., Guerrero F., Ruíz J. and García-Lafuente J.; 2005: *Variability in the spatio-temporal distribution and size-structure of phytoplankton across an upwelling area in the NW-Alboran Sea (W-Mediterranean)*. Cont. Shelf Res., 25, 589-608, doi: 10.1016/j.csr.2004.09.016.
- Reynolds R.M.; 1993: *Physical oceanography of the Gulf, Strait of Hormuz, and the Gulf of Oman - Results from the Mt Mitchell expedition*. Mar. Pollut. Bull., 27, 35-59.
- Schwing F.B., O'Farrell M., Steger J.M. and Baltz K.; 1996: *Coastal upwelling indices west coast of North America*. U.S. Department of Commerce, NOAA Technical Memorandum NMFS, NOAA-TM-NMFS-SWFSC-231, Tech. Report, 35 pp.

- Shankar D., Vinayachandran P. and Unnikrishnan A.; 2002: *The monsoon currents in the north Indian Ocean*. Prog. Oceanogr., 52, 63-120.
- Smitha B.R., Sanjeevan V.N., Padmakumar K.B., Hussain M.S., Salini T.C. and Lix J.K.; 2022: *Role of mesoscale eddies in the sustenance of high biological productivity in north eastern Arabian Sea during the winter-spring transition period*. Sci. Total Environ. 809, 151173, 46 pp., doi: 10.1016/j.scitotenv.2021.151173.
- Sousa M.C., Ribeiro A., Des M., Gomez-Gesteira M., deCastro M. and Dias J.M.; 2020: *NW Iberian Peninsula coastal upwelling future weakening: competition between wind intensification and surface heating*. Sci. Total Environ., 703, 134808, 10 pp., doi: 10.1016/j.scitotenv.2019.134808.
- Sudre J., Maes C. and Garçon V.; 2013: *On the global estimates of geostrophic and Ekman surface currents*. Limnol. Oceanogr.: Fluids Environ., 3, 1-20, doi: 10.1215/21573689-2071927.
- Tomczak M. and Godfrey J.S.; 2003: *Regional oceanography: an introduction, 2nd ed.* Daya Publishing House, Delhi, India, 390 pp., doi: 10.5860/choice.32-0321
- Trinchin R., Ortega L. and Barreiro M.; 2019: *Spatiotemporal characterization of summer coastal upwelling events in Uruguay, south America*. Regional Stud. Mar. Sci., 31, 100787, ?? pp., doi: 10.1016/j.rsma.2019.100787.
- Varela R., Santos F., Gómez-Gesteira M., Álvarez I., Costoya X. and Días J.M.; 2016: *Influence of coastal upwelling on SST trends along the south coast of Java*. PloS One, 11, e0162122, 14 pp., doi: 10.1371/journal.pone.0162122.
- Varela R., Lima F.P., Seabra R., Meneghesso C. and Gómez-Gesteira M.; 2018: *Coastal warming and wind-driven upwelling: a global analysis*. Sci. Total Environ., 639, 1501-1511, doi: 10.1016/j.scitotenv.2018.05.273.
- Vic C., Capet X., Rouillet G. and Carton X.; 2017: *Western boundary upwelling dynamics off Oman*. Ocean Dyn., 67, 585-595, doi: 10.1007/s10236-017-1044-5.
- Vinayachandran P.N.; 2004: *Summer cooling of the Arabian Sea during contrasting monsoons*. Geophys. Res. Lett., 31, L13306, 5 pp., doi: 10.1029/2004GL019961.
- Vinayachandran P.N.M., Masumoto Y., Roberts M.J., Jenny A., Huggett J.A., Halo I., Chatterjee A., Amol P., Gupta G.V.M., Singh A., Mukherjee A., Prakash S., Beckley L.E., Raes E.J. and Hood R.; 2021: *Reviews and syntheses: physical and biogeochemical processes associated with upwelling in the Indian Ocean*. Biogeosci., 18, 5967-6029, doi: 10.5194/bg-18-5967-2021.
- Vinod Kumar K., Seemanth M., Vethamony P. and Aboobacker V.M.; 2014: *On the spatial structure and time evolution of shamal winds over the Arabian Sea - a case study through numerical modelling*. Int. J. Climatol., 34, 2122-2128, doi: 10.1002/joc.3819.
- Wang B., Wu R. and Lau K.; 2001: *Interannual variability of the Asian summer monsoon: contrasts between the Indian and the western North Pacific - East Asian monsoons*. J. Clim., 14, 4073-4090.
- Watson R. and Pauly D.; 2001: *Systematic distortions in world fisheries catch trends*. Nat., 414, 534-536.
- Wessel P. and Smith W.H.; 1996: *A global, self-consistent, hierarchical, high-resolution shoreline database*. J. Geophys. Res.: Solid Earth, 101, 8741-8743.
- Zavala-Hidalgo J., Gallegos-García A., Martínez-López B., Morey S.L. and O'Brien J.J.; 2006: *Seasonal upwelling on the western and southern shelves of the Gulf of Mexico*. Ocean Dyn., 56, 333-338, doi: 10.1007/s10236-006-0072-3.

Corresponding author: Mojtaba Zoljoodi Zarandi
 Department of Marine Meteorology & Physical Oceanography,
 Atmospheric Science and Meteorological Research Center (ASMERC)
 Pajooesh Blvd., Shahid Kharrazi Highway, 14155-4781 Tehran, Iran
 Phone: +98 21 4478 7652; e-mail: m-zoljodi@irimo.ir